Spin-Valley Half-Metal as a Prospective Material for Spin Valleytronics

A. V. Rozhkov,[1,2,3] A. L. Rakhmanov,[1,3,2,4] A. O. Sboychakov,[1,2] K. I. Kugel,[2,5] and Franco Nori[1,6]
[1]Center for Emergent Matter Science, RIKEN, Wako-shi, Saitama 351-0198 Japan
[2]Institute for Theoretical and Applied Electrodynamics, Russian Academy of Sciences, Moscow 125412 Russia
[3]Moscow Institute for Physics and Technology (State University), Dolgoprudnyi 141700 Russia
[4]Dukhov Research Institute of Automatics, Moscow 127055 Russia
[5]National Research University Higher School of Economics, Moscow 101000 Russia
[6]Department of Physics, University of Michigan, Ann Arbor, Michigan 48109-1040, USA
(Received 11 April 2017; published 8 September 2017)

Half-metallicity (full spin polarization of the Fermi surface) usually occurs in strongly correlated electron systems. We demonstrate that doping a spin-density wave insulator in the weak-coupling regime may also stabilize half-metallic states. In the absence of doping, the spin-density wave is formed by four nested bands [i.e., each band is characterized by charge (electron or hole) and spin (up or down) labels]. Of these four bands, only two accumulate the charge carriers introduced by doping, forming a half-metallic two-valley Fermi surface. Depending on the parameters, the spin polarizations of the electronlike and holelike valleys may be either (i) parallel or (ii) antiparallel. The Fermi surface of (i) is fully spin polarized (similar to usual half-metals). Case (ii), referred to as "a spin-valley half-metal," corresponds to complete polarization with respect to the spin-valley operator. The properties of these states are discussed.

DOI: 10.1103/PhysRevLett.119.107601

Introduction.—Half-metallicity [1–3] is a useful property for spintronics applications. Unlike usual metals, which have both spin projections (spin-up and spin-down) on the Fermi surface, half-metallicity implies that electrons with only one spin projection, for example, spin-up, reach the Fermi level, while spin-down states are pushed away from the Fermi energy. A highly desirable consequence [3,4] of half-metallicity is the perfect spin polarization of the current. Experiments confirmed that many real materials are half-metals, for example, NiMnSb [5], $(La_{0.7}Sr_{0.3})MnO_3$ [6], CrO_2 [7], Co_2MnSi [8], and others. From the theory standpoint, the half-metallicity of these compounds relies on sizable electron-electron interactions, associated with transition-metal atoms. However, in recent years, the search for "metal-free half-metals" began [9,10]. Such systems could be useful for biocompatible applications and, in general, are consistent with current interest in carbon-based and organic-based mesoscopic systems [11–16]. It is difficult to expect a strong electron-electron interaction for systems composed entirely of s and p elements. Thus, different mechanisms for half-metallicity must be looked for. In this Letter, we discuss a novel possibility to generate half-metallicity. Specifically, we demonstrate that doping a spin-density wave (SDW) or charge-density wave (CDW) insulator may stabilize a certain type of half-metallic state. Let the undoped system [see Fig. 1(a)] have two nested Fermi surface sheets, which we will also refer to as valleys. Let one sheet, or valley, correspond to electron states and another to hole states. Both valleys are spin degenerate. The SDW or CDW instability opens a gap generating an insulating ground state [Fig. 1(b)]. We show that, when doping is introduced, each valley becomes half-metallic. If the spin polarizations of both sheets are parallel to each other [Fig. 1(c)], a half-metallic state, called below the CDW half-metal, emerges. For antiparallel polarizations [Fig. 1(d)], a different half-metallic state, the spin-valley half-metal, appears. The properties of these two states are discussed below.

Model.—Our model describes two bands, or valleys: an electronic band a and a hole band b, shown as blue and red parabolas, respectively, in Fig. 1(a), with the following single-particle dispersions ($\hbar = 1$):

$$\varepsilon^a(\mathbf{k}) = \frac{\mathbf{k}^2}{2m_a} + \varepsilon^a_{\min} - \mu, \qquad \varepsilon^a_{\min} < \varepsilon^a < \varepsilon^a_{\max}, \quad (1)$$

$$\varepsilon^b(\mathbf{k}+\mathbf{Q}_0) = -\frac{\mathbf{k}^2}{2m_b} + \varepsilon^b_{\max} - \mu, \quad \varepsilon^b_{\min} < \varepsilon^b < \varepsilon^b_{\max}. \quad (2)$$

Here band a is centered at $\mathbf{k} = 0$ and band b at some finite momentum $\mathbf{Q}_0$. Below, for simplicity, we assume the perfect electron-hole symmetry: $m_a = m_b = m$ and $\varepsilon^b_{\max} = -\varepsilon^a_{\min} = \varepsilon_F$; consequently, $\varepsilon^a(\mathbf{k}) = -\varepsilon^b(\mathbf{k}+\mathbf{Q}_0) = \varepsilon_{\mathbf{k}}$. Zero doping corresponds to $\mu = 0$. Undoped Fermi surface sheets for the a and b bands are characterized by a single Fermi momentum $k_F = \sqrt{2m\varepsilon_F}$, and density of states (per spin projection) $N_F = mk_F/(2\pi^2)$ at the Fermi energy. This provides a perfect nesting: a translation of the electron Fermi surface by the vector $\mathbf{Q}_0$ completely superposes the sheets. The total Hamiltonian is equal to

$$\hat{H} = \hat{H}_e + \hat{H}_{\text{int}}, \quad (3)$$

 © 2017 American Physical Society

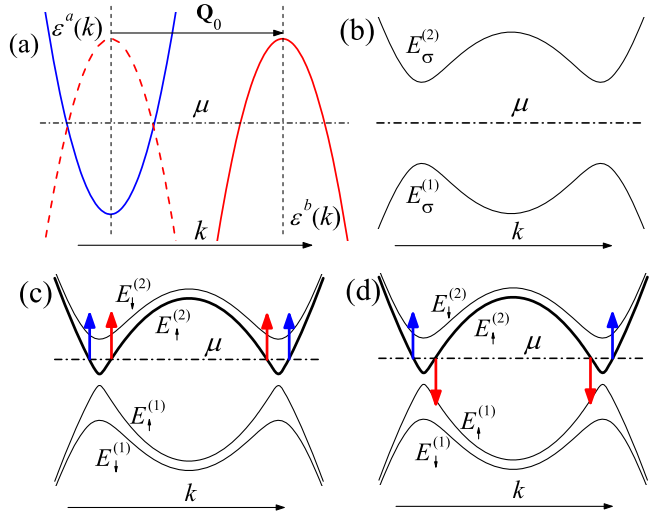

FIG. 1. The electron bands and spin structure for different dopings x [the vertical (horizontal) axis is energy (momentum), and the Fermi level μ is shown by horizontal dash-dot lines]. (a) Noninteracting bands at $x = 0$. The bands are shown by solid curves; the dashed parabola is the hole band translated by the nesting vector $\mathbf{Q}_0$. (b)–(d) The interaction is taken into account. (b) If $x = 0$, the ground state is an insulating SDW or CDW, with degenerate sectors ($\Delta_\uparrow \equiv \Delta_\downarrow$), with electron bands $E_\sigma^{(1,2)}$ given by Eq. (9). (c), (d) If $x > 0$, the sectors are no longer degenerate ($\Delta_\uparrow < \mu < \Delta_\downarrow \equiv \Delta_0$), with the charge accumulating in sector "↑," in which a Fermi surface opens. The spin polarizations (arrows) of the Fermi surface sheets correspond to (c) the CDW half-metal and (d) the spin-valley half-metal.

where $\hat{H}_e$ is the single-electron term, described by the dispersions (1) and (2), while $\hat{H}_{\rm int}$ corresponds to the interaction between quasiparticles.

To treat the SDW instability, it is sufficient to keep in $H_{\rm int}$ only the interaction between electrons in the a and b bands. We also assume that the interaction is a short-range one. Let us initially focus on the following interaction term (the neglected term will be discussed later):

$$\hat{H}_{\rm int} = g \int d^3\mathbf{r} \sum_{\sigma\sigma'} \psi^\dagger_{a\sigma}(\mathbf{r})\psi_{a\sigma}(\mathbf{r})\psi^\dagger_{b\sigma'}(\mathbf{r})\psi_{b\sigma'}(\mathbf{r}). \quad (4)$$

Here, $\psi_{a\sigma}$ denotes the usual fermionic field operator for band α and spin σ; the symbol $\mathbf{r}$ refers to spatial coordinates. The interaction is repulsive ($g > 0$) and weak ($gN_F \ll 1$).

Spin-valley half-metal.—When the Fermi surface sheets of the holes and the electrons perfectly match each other, model (3) describes the spontaneous formation of SDW or CDW orders. We start with the SDW. The SDW ground state is believed to be unique (up to rotations of the spin-polarization axis) and well described by a BCS-like theory. The electron operators can be grouped into two sectors, labeled by the index $\sigma = \pm 1$: sector σ consists of $\psi_{a\sigma}$ and $\psi_{b\bar{\sigma}}$ (here $\bar{\sigma}$ means $-\sigma$). In the mean-field approach, the sectors are decoupled, and the SDW order parameter can be written as

$$\Delta_\sigma = \frac{g}{V}\sum_{\mathbf{k}} \langle \psi^\dagger_{\mathbf{k}a\sigma}\psi_{\mathbf{k}b\bar{\sigma}}\rangle, \quad (5)$$

where V is the system volume and $\langle \ldots \rangle$ denotes the diagonal matrix element for the ground state. At zero doping, the sectors are degenerate: $\Delta_\uparrow = \Delta_\downarrow = \Delta_0$, where $\Delta_0 \approx \varepsilon_F \exp(-1/gN_F)$ is the order parameter at perfect nesting [see Fig. 1(b)]. This equality implies that the SDW polarization in real space is directed along the x axis:

$$\langle S^x(\mathbf{r})\rangle = \frac{\Delta_\uparrow + \Delta_\downarrow}{g}\cos(\mathbf{Q}_0\mathbf{r}) = \frac{2\Delta_0}{g}\cos(\mathbf{Q}_0\mathbf{r}), \quad (6)$$

$$\langle S^y(\mathbf{r})\rangle = \frac{\Delta_\uparrow - \Delta_\downarrow}{2g}\sin(\mathbf{Q}_0\mathbf{r}) \equiv 0. \quad (7)$$

Doping destroys the perfect nesting, and the number of low-energy states competing to become the true ground state increases. Both incommensurate and inhomogeneous phases [17–25] were considered for Hamiltonian (3) and its modifications. Here we argue that the half-metallic state is yet another viable contender in the case of imperfect nesting.

The grand potential of our system Ω at zero temperature and finite doping x is a sum of two partial grand potentials $\Omega = \sum_\sigma \Omega_\sigma$, where

$$\Omega_\sigma = \frac{\Delta_\sigma^2 V}{g} - \sum_{\mathbf{k}} \left[\mu - E^{(1)}_{\mathbf{k}\sigma} + \left(\mu - E^{(2)}_{\mathbf{k}\sigma}\right)\theta\left(\mu - E^{(2)}_{\mathbf{k}\sigma}\right)\right], \quad (8)$$

$$E^{(1,2)}_{\mathbf{k}\sigma} = \mp\sqrt{\varepsilon^2_{\mathbf{k}} + \Delta^2_\sigma}, \qquad \theta(z) \text{ is the step function.} \quad (9)$$

Here we assume that $\mu > 0$. To describe doping, it is convenient to introduce the partial dopings $x_\sigma = -\partial\Omega_\sigma/\partial\mu$, which are the amounts of charge accumulated in sectors σ. Parameter Δ_σ minimizes $\Omega_\sigma(\Delta_\sigma)$. Thus, one has to solve

$$\frac{\partial\Omega_\sigma}{\partial\Delta_\sigma} = 0, \qquad x_\uparrow + x_\downarrow = x, \quad (10)$$

to determine μ and Δ_σ. Equations (8) and (10) are valid provided that the state remains homogeneous and the SDW order remains commensurate even at finite doping.

Since the two sectors σ are decoupled, one can calculate [18,25,26] parameters Δ_σ and μ as functions of x_σ:

$$\Delta_\sigma = \Delta_0\sqrt{1 - \frac{x_\sigma}{N_F\Delta_0}} \quad \text{and} \quad \mu = \Delta_0 - \frac{x_\sigma}{2N_F}. \quad (11)$$

We see that the doping destroys the ordered state, and the homogeneous commensurate state becomes completely unstable for $x_\sigma > x_c = N_F\Delta_0$.

It is often implicitly assumed (e.g., Refs. [17,25,26]) that the charge carriers are spread evenly between both sectors

($x_\uparrow = x_\downarrow$) and the degeneracy of Δ_σ persists even for finite x. Yet, it is easy to show that the spontaneous lifting of this degeneracy optimizes the energy. To prove this, consider the system free energy $F = \sum_\sigma F_\sigma$, where the partial free energy $F_\sigma = \Omega_\sigma + \mu x_\sigma$ can be calculated as $F_\sigma(x_\sigma) = F_\sigma(0) + \int_0^{x_\sigma} dx' \mu(x')$, to obtain

$$\frac{F}{V} = \sum_\sigma \frac{F_\sigma}{V} = -N_F\Delta_0^2 + \Delta_0 x - \frac{x_\uparrow^2 + x_\downarrow^2}{4N_F}, \qquad (12)$$

where we took into account that $F_\sigma(0) = -N_F\Delta_0^2/2$. Only the third term in Eq. (12) depends on the distribution of the charge among the two sectors. It is easy to check that, if $x_\sigma = x$ and $x_{\bar\sigma} = 0$, the third term, together with F, is the smallest. In other words, for fixed x, the most stable spatially homogeneous state of the model corresponds to the case when all the doped charge is accumulated in a given sector. The other sector is completely free of the extra charge carriers. Therefore,

$$\frac{F}{V} = -N_F\Delta_0^2 + \Delta_0 x - \frac{x^2}{4N_F}, \qquad (13)$$

$$\mu = \Delta_0 - \frac{x}{2N_F}, \qquad (14)$$

$$\Delta_\sigma(x) = \Delta_0\sqrt{1 - \frac{x}{N_F\Delta_0}}, \qquad \Delta_{\bar\sigma}(x) = \Delta_0. \qquad (15)$$

These relations are valid for not too strong doping $x < N_F\Delta_0$. An important feature of Eq. (13) is that the second derivative $\partial^2 F/\partial x^2$ is negative. This means that the doped system is unstable with respect to electronic phase separation [18,22,23,26–30]. However, the long-range Coulomb interaction can suppress the phase separation [31,32]. Thus, it is reasonable to study the properties of the homogeneous state [33].

It follows from Eqs. (14) and (15) that $\Delta_\sigma(x) < \mu(x) < \Delta_{\bar\sigma}(x) = \Delta_0$, when $x > 0$. This means that, in the sector $\bar\sigma$, the order parameter remains equal to Δ_0. Since the chemical potential is lower than $\Delta_{\bar\sigma}$, no charge enters sector $\bar\sigma$; see Fig. 1(d). In the sector σ, two Fermi surface sheets emerge. They are fixed by the equation $\varepsilon_{\mathbf{k}}^2 = [\mu(x)]^2 - [\Delta_\sigma(x)]^2$, which is equivalent to $\varepsilon_{\mathbf{k}} = \pm x/2N_F$. As the doped charges are distributed unevenly between the sectors, the doped state acquires nontrivial macroscopic quantum numbers. To characterize the macroscopic state, it is useful to specify spin operator $\hat S = \sum_{\alpha\sigma}\sigma\hat N_{\alpha\sigma}$ and spin-valley operator $\hat S_v = \sum_{\alpha\sigma}\sigma v_\alpha\hat N_{\alpha\sigma}$. Here, $\alpha = a, b$, is the valley label and v_α is defined as $v_a = 1$, $v_b = -1$. The operator $\hat N_{\alpha\sigma} = \sum_{\mathbf{k}}\psi^\dagger_{\mathbf{k}\alpha\sigma}\psi_{\mathbf{k}\alpha\sigma}$ corresponds to the number of electrons with spin σ in valley α. The Hamiltonian (3) commutes with both $\hat S$ and $\hat S_v$. The field operators satisfy obvious commutation rules $[\hat S, \psi_{\alpha\sigma}] = \sigma\psi_{\alpha\sigma}$ and $[\hat S_v, \psi_{\alpha\sigma}] = \sigma v_\alpha\psi_{\alpha\sigma}$. Namely, in addition to the spin quantum number σ, a field $\psi_{\alpha\sigma}$ can be characterized by the spin-valley projection σv_α.

It is easy to check that in the sector σ both $\psi_{a\sigma}$ and $\psi_{b\bar\sigma}$ carry the same spin-valley quantum equal to $+\sigma$. In the sector $\bar\sigma$, the field operators correspond to a $-\sigma$ quantum of $\hat S_v$. That is, the Fermi surface of the doped system is characterized by the single projection of the spin-valley operator. The Fermi surface sheets with the opposite projection of $\hat S_v$ are absent, since the sector $\bar\sigma$ is gapped. Thus, the doped system can be referred to as *a spin-valley half-metal*: like a classical half-metal, our system exhibits complete polarization of the Fermi surface; however, in contrast to the usual half-metal, the polarization is not the spin polarization but, rather, the spin-valley one. Therefore, the electric current through the spin-valley half-metal is completely spin-valley polarized.

Since the sector $\bar\sigma$ is free of doped electrons, the average values of $\hat N_{a\bar\sigma}$ and $\hat N_{b\sigma}$ remain unaffected by the doping, while $\langle\hat N_{a\sigma}\rangle$ and $\langle\hat N_{b\bar\sigma}\rangle$ change. Taking the average occupation numbers $N_{\alpha\sigma} = \langle\hat N_{\alpha\sigma}\rangle$ in the undoped state to be zero, we can write $N_{a\bar\sigma} = N_{b\sigma} = 0$, and $N_{a\sigma} + N_{b\bar\sigma} = xV$. Consequently, $S_v = \langle\hat S_v\rangle$ is proportional to x. Namely, $S_v = \sigma xV$. In a system with perfect electron-hole symmetry, we have $N_{a\sigma} = N_{b\bar\sigma} = xV/2$, which corresponds to $S = \langle\hat S\rangle \equiv 0$, for any x. If the symmetry is absent, then $|S| \propto x$. However, the net spin polarization of the spin-valley half-metal satisfies the inequality $|S| < |S_v|$.

Doping also affects the SDW order inherited from the undoped state. Intuitively, since the charge enters only one of the two sectors, the symmetry between sectors σ disappears for $x > 0$. [Equations (15) prove this.] The simple SDW is replaced by a more complicated order parameter: analyzing Eqs. (6) and (7) one can prove that, at finite doping, a circularly polarized spin component emerges $\{\delta S^x(\mathbf{r}), \delta S^y(\mathbf{r})\} \propto (\Delta_\uparrow - \Delta_\downarrow)\{\cos(\mathbf{Q}_0\mathbf{r}), \sin(\mathbf{Q}_0\mathbf{r})\}$. The amplitude of this component increases when x grows.

From spin-valley half-metal to CDW half-metal.— In addition to the expected invariance with respect to simultaneous rotations of all fermion spins, our model Hamiltonian allows for a broader class of symmetries: it remains unchanged, even if the electron and hole spins are transformed by two different rotation operators. This observation can be trivially proven in the absence of interaction ($g = 0$). In the case of a generic interaction, this symmetry does not apply. However, if the interaction is short-range, as in Eq. (4), the invariance of the Hamiltonian under such transformations remains. Indeed, the integrand in Eq. (4) is $\propto \rho_e\rho_h$, where ρ_e and ρ_h are the density operators for electrons and holes, respectively, which both are invariant under separate rotations of the electron and hole spins. Therefore, the substitution

$$\psi_{b\uparrow} \to \psi_{b\downarrow}, \qquad \psi_{b\downarrow} \to \psi_{b\uparrow} \qquad (16)$$

corresponds to a symmetry of the model. Thus, Eq. (16) either preserves the ground state or transforms one ground

state into another one. Since the order parameter [Eq. (5)] changes under the transformation (16), we must conclude that a new ground state is generated by such a substitution. If we start with the spin-valley half-metal ground state, what kind of new state does the transformation (16) bring us?

Consider the SDW polarization [Eq. (6)] at zero doping. Under the transformation (16), the SDW is replaced by a CDW with a finite average value for the density operator $\hat{\rho}_{\mathbf{Q}_0}$: $\langle \hat{S}^x_{\mathbf{Q}_0} \rangle = \sum_\sigma \langle \psi^\dagger_{\mathbf{k}a\sigma} \psi_{\mathbf{k}b\bar{\sigma}} \rangle \to \sum_\sigma \langle \psi^\dagger_{\mathbf{k}a\sigma} \psi_{\mathbf{k}b\sigma} \rangle = \langle \hat{\rho}_{\mathbf{Q}_0} \rangle$. Calculations identical (up to relabeling) to the case of the SDW order demonstrate that for $x > 0$ the charge carriers accumulate in a single mean-field sector. However, the sector composition is changed by the transformation (16): sector σ consists of $\psi_{a\sigma}$ and $\psi_{b\sigma}$. Unlike the case of spin-valley half-metals, now both electronic fields within a single sector have the same spin projection. Therefore, if the doped charge enters sector σ, both Fermi surface sheets have identical spin polarizations equal to σ; see Fig. 1(c). This perfect polarization of the Fermi surface is a hallmark feature of half-metals. Thus, the spin-valley half-metal is related to the CDW half-metal by the substitution (16), and both states are degenerate within our model. This relation becomes apparent if we notice that (16) switches the operators $\hat{S}$ and $\hat{S}_v$. Consequently, in the CDW half-metal $S = \sigma x V$ and $|S_v| < |S|$. When $x > 0$, in addition to the CDW order parameter, the SDW order parameter $\langle S^z_{\mathbf{Q}_0} \rangle$ is generated. It grows monotonically with x.

Note, however, that the degeneracy between the SDW and CDW ground states is an artifact of the short-range interaction [Eq. (4)], which possesses extra symmetries absent in more realistic models. The effects of more generic interaction operators are discussed below.

Discussion.—While the mechanism presented here is quite general and may be relevant to any material with a nesting-driven density wave, below we will overview some extensions of the model, which may affect the proposed half-metallic states. Specifically, the interaction Eq. (4) is not the most general form of electron-electron coupling. In particular, the "exchange" term $\hat{H}_{\text{ex}} = g_\perp \int d^3x \sum_{\sigma\sigma'} \psi^\dagger_{a\sigma} \psi_{b\sigma} \psi^\dagger_{b\sigma'} \psi_{a\sigma'}$ should be accounted for. The coupling constant $g_\perp > 0$ describes a repulsive interaction at finite momentum $\mathbf{Q}_0$. The exchange term $\hat{H}_{\text{ex}}$ immediately lifts the degeneracy between the SDW and CDW, in favor of SDW. This means that, for finite doping, the spin-valley half-metal is more stable than the CDW half-metal. On the other hand, other factors could favor the CDW half-metal, for example, the proximity to a lattice instability. An external magnetic field acts similarly, since the total spin of the CDW half-metal exceeds the spin of the spin-valley half-metal.

We assumed that the Coulomb interaction guarantees the homogeneity of the electron liquid [33]. Thus, in the above discussion, we neglected the possibility of phase separation. In addition, the incommensurate SDW states were not considered. While the detailed study of such states is an interesting goal for future research, we do not expect that this modification would affect significantly the stability of the half-metallic phases, at least at some doping range. Indeed, at the mean-field level the free energy in the presence of the incommensurate SDW equals $F^{\text{ic}}(x) = \min_{x_\uparrow + x_\downarrow = x} [F^{\text{ic}}_0(x_\uparrow) + F^{\text{ic}}_0(x_\downarrow)]$, where $F^{\text{ic}}_0(x_\sigma)$ is the free energy of a sector with partial doping x_σ. As above, the free energy of the system is found by minimization under the condition $x_\uparrow + x_\downarrow = x$. We calculated $F^{\text{ic}}_0(x_\sigma)$ numerically, as described in Ref. [26]. Our analysis shows that $\partial^2 F^{\text{ic}}_0(x_\sigma)/\partial x^2_\sigma < 0$ for x_σ less than the threshold value $x^* \cong 0.83 N_F \Delta_0$. This is a rather general feature of a system with imperfect nesting [18,22,23,26,30]. Since the second derivative of F^{ic}_0 is negative, the sum $F^{\text{ic}}_0(x_\uparrow) + F^{\text{ic}}_0(x - x_\uparrow)$ as a function of $x_\uparrow \in [0, x]$ is concave. Consequently, the extremum of the latter sum at $x_\uparrow = x/2$ corresponds to a maximum, not a minimum (see Fig. 2). Therefore, the total free energy is minimized as follows: $F^{\text{ic}}(x) = F^{\text{ic}}_0(x) + F^{\text{ic}}_0(0)$, at $x_\sigma = x$ and $x_{\bar{\sigma}} = 0$. Thus, the undoped sector $\bar{\sigma}$ remains insulating. All doped charge goes to sector σ, which becomes metallic, with a well-defined Fermi surface, and we recover the spin-valley half-metal with an incommensurate SDW.

If $x_\sigma > x^*$, then $\partial^2 F^{\text{ic}}_0(x_\sigma)/\partial x^2_\sigma > 0$, and the total free energy $F^{\text{ic}}_0(x_\sigma) + F^{\text{ic}}_0(x - x_\sigma)$ acquires a local minimum at $x_\uparrow = x_\downarrow = x/2$ (see Fig. 2). When doping increases even further, this minimum becomes a global minimum for $x \cong 1.8 N_F \Delta_0$. Consequently, the first-order transition from incommensurate spin-valley half-metal to common incommensurate SDW phase occurs at this point.

We assume that both the electron and hole sheets in the Fermi surface are perfectly nested at zero doping. Generally, the sheets have nonidentical shapes, causing finite denesting. For example, one sheet may be spherical, while the other may be elliptical [23]. At moderate denesting, the range of

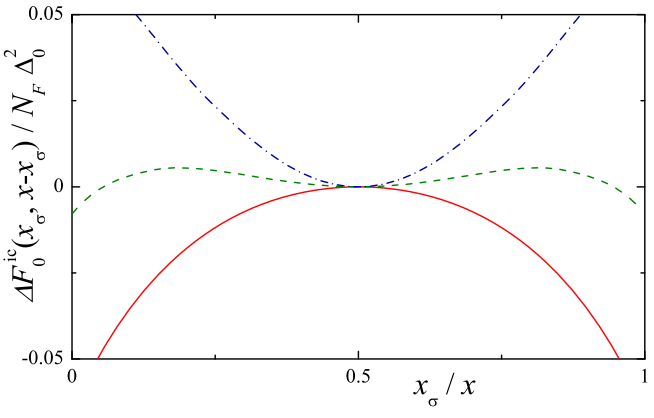

FIG. 2. Dependence of $\Delta F^{\text{ic}}_0(x_\sigma, x - x_\sigma) \equiv F^{\text{ic}}_0(x_\sigma) + F^{\text{ic}}_0(x - x_\sigma) - 2F^{\text{ic}}_0(x/2)$ on the partial doping x_σ, calculated at $T = 0$ and fixed total doping $x = 1.4 N_F \Delta_0$ [(red) solid curve], $x = 1.76 N_F \Delta_0$ [(green) dashed curve], and $x = 2.0 N_F \Delta_0$ [(blue) dash-dot curve].

doping where $\partial^2 F_0^{\rm ic}(x)/\partial x^2 < 0$ diminishes [23]. When the sheet shapes differ significantly, one has $\partial^2 F_0^{\rm ic}(x)/\partial x^2 > 0$ for all x, and the half-metal states become impossible. On the other hand, if the sheets are nonspherical, but the zero-doping nesting is preserved (at $x = 0$ the sheets are identical), our conclusions endure, and only minor mathematical modifications to the formalism (the density of states acquires a dependence on the spherical angles) are required. We also neglected several other perturbations (disorder, spin-orbit coupling, and umklapp processes). The stability of the half-metal phases against these should be checked in the future.

In conclusion, we demonstrated that doping a SDW state with perfectly nested Fermi surface sheets stabilizes a half-metal-like ground state. Depending on the microscopic parameters and the external magnetic field, such a ground state could be either a CDW half-metal with complete spin polarization of the Fermi surface or a spin-valley half-metal. The Fermi surface of the latter state is characterized by a perfect polarization in the spin-valley space. While the CDW half-metal supports purely spin-polarized currents, which is a natural consequence of the Fermi surface polarization, the spin-valley half-metal supports spin-valley-polarized currents. The proposed scheme is a controllable weak-coupling approach to half-metallicity. The discussed mechanism may be of importance for the current search for nontoxic biologically compatible materials with nontrivial electronic properties.

This work is partially supported by the Russian Foundation for Basic Research (Projects No. 17-02-00323 and No. 15-02-02128), the RIKEN iTHES Project, the RIKEN-AIST "Challenge Research" program, MURI Center for Dynamic Magneto-Optics via the AFOSR Grant No. FA9550-14-1-0040, the Japan Society for the Promotion of Science (KAKENHI), the IMPACT program of JST, JSPS-RFBR Grant No. 17-52-50023, CREST Grant No. JPMJCR1676, and the Sir John Templeton Foundation.

[1] R. A. de Groot, F. M. Mueller, P. G. van Engen, and K. H. J. Buschow, New Class of Materials: Half-Metallic Ferromagnets, Phys. Rev. Lett. **50**, 2024 (1983).
[2] M. I. Katsnelson, V. Y. Irkhin, L. Chioncel, A. I. Lichtenstein, and R. A. de Groot, Half-metallic ferromagnets: From band structure to many-body effects, Rev. Mod. Phys. **80**, 315 (2008).
[3] X. Hu, Half-metallic antiferromagnet as a prospective material for spintronics, Adv. Mater. **24**, 294 (2012).
[4] I. Źutić, J. Fabian, and S. Das Sarma, Spintronics: Fundamentals and applications, Rev. Mod. Phys. **76**, 323 (2004).
[5] K. E. H. M. Hanssen, P. E. Mijnarends, L. P. L. M. Rabou, and K. H. J. Buschow, Positron-annihilation study of the half-metallic ferromagnet NiMnSb: Experiment, Phys. Rev. B **42**, 1533 (1990).
[6] J.-H. Park, E. Vescovo, H.-J. Kim, C. Kwon, R. Ramesh, and T. Venkatesan, Direct evidence for a half-metallic ferromagnet, Nature (London) **392**, 794 (1998).
[7] Y. Ji, G. J. Strijkers, F. Y. Yang, C. L. Chien, J. M. Byers, A. Anguelouch, G. Xiao, and A. Gupta, Determination of the Spin Polarization of Half-Metallic CrO_2 by Point Contact Andreev Reflection, Phys. Rev. Lett. **86**, 5585 (2001).
[8] M. Jourdan *et al.*, Direct observation of half-metallicity in the Heusler compound Co_2MnSi, Nat. Commun. **5**, 3974 (2014).
[9] A. Du, S. Sanvito, and S. C. Smith, First-Principles Prediction of Metal-Free Magnetism and Intrinsic Half-Metallicity in Graphitic Carbon Nitride, Phys. Rev. Lett. **108**, 197207 (2012).
[10] A. Hashmi and J. Hong, Metal free half metallicity in 2D system: Structural and magnetic properties of g-C_4N_3 on BN, Sci. Rep. **4**, 4374 (2014).
[11] D. Soriano and J. Fernández-Rossier, Spontaneous persistent currents in a quantum spin Hall insulator, Phys. Rev. B **82**, 161302 (2010).
[12] H. Klauk, Organic thin-film transistors, Chem. Soc. Rev. **39**, 2643 (2010).
[13] P. Avouris, Z. Chen, and V. Perebeinos, Carbon-based electronics, Nat. Nanotechnol. **2**, 605 (2007).
[14] A. Rozhkov, G. Giavaras, Y. P. Bliokh, V. Freilikher, and F. Nori, Electronic properties of mesoscopic graphene structures: Charge confinement and control of spin and charge transport, Phys. Rep. **503**, 77 (2011).
[15] W. Sa-Ke, T. Hong-Yu, Y. Yong-Hong, and W. Jun, Spin and valley half metal induced by staggered potential and magnetization in silicene, Chin. Phys. B **23**, 017203 (2014).
[16] A. Rozhkov, A. Sboychakov, A. Rakhmanov, and F. Nori, Electronic properties of graphene-based bilayer systems, Phys. Rep. **648**, 1 (2016).
[17] T. M. Rice, Band-structure effects in itinerant antiferromagnetism, Phys. Rev. B **2**, 3619 (1970).
[18] A. Gorbatsevich, Y. Kopaev, and I. Tokatly, Band theory of phase stratification, Zh. Eksp. Teor. Fiz. **101**, 971 (1992) [Sov. Phys. JETP **74**, 521 (1992)].
[19] I. Eremin and A. V. Chubukov, Magnetic degeneracy and hidden metallicity of the spin-density-wave state in ferropnictides, Phys. Rev. B **81**, 024511 (2010).
[20] A. L. Rakhmanov, A. V. Rozhkov, A. O. Sboychakov, and F. Nori, Instabilities of the *AA*-Stacked Graphene Bilayer, Phys. Rev. Lett. **109**, 206801 (2012).
[21] A. O. Sboychakov, A. V. Rozhkov, A. L. Rakhmanov, and F. Nori, Antiferromagnetic states and phase separation in doped AA-stacked graphene bilayers, Phys. Rev. B **88**, 045409 (2013).
[22] A. O. Sboychakov, A. L. Rakhmanov, A. V. Rozhkov, and F. Nori, Metal-insulator transition and phase separation in doped AA-stacked graphene bilayer, Phys. Rev. B **87**, 121401 (2013).
[23] A. O. Sboychakov, A. V. Rozhkov, K. I. Kugel, A. L. Rakhmanov, and F. Nori, Electronic phase separation in iron pnictides, Phys. Rev. B **88**, 195142 (2013).
[24] R. S. Akzyanov, A. O. Sboychakov, A. V. Rozhkov, A. L. Rakhmanov, and F. Nori, *AA*-stacked bilayer graphene in an applied electric field: Tunable antiferromagnetism and coexisting exciton order parameter, Phys. Rev. B **90**, 155415 (2014).

[25] A. O. Sboychakov, A. L. Rakhmanov, K. I. Kugel, A. V. Rozhkov, and F. Nori, Magnetic field effects in electron systems with imperfect nesting, Phys. Rev. B **95**, 014203 (2017).

[26] A. L. Rakhmanov, A. V. Rozhkov, A. O. Sboychakov, and F. Nori, Phase separation of antiferromagnetic ground states in systems with imperfect nesting, Phys. Rev. B **87**, 075128 (2013).

[27] A. Moreo, S. Yunoki, and E. Dagotto, Phase separation scenario for manganese oxides and related materials, Science **283**, 2034 (1999).

[28] E. Dagotto, *Nanoscale Phase Separation and Colossal Magnetoresistance*, Springer Series in Solid-State Sciences (Springer, Berlin, 2003).

[29] E. Dagotto, J. Burgy, and A. Moreo, Nanoscale phase separation in colossal magnetoresistance materials: Lessons for the cuprates?, Solid State Commun. **126**, 9 (2003).

[30] P. A. Igoshev, M. A. Timirgazin, A. A. Katanin, A. K. Arzhnikov, and V. Y. Irkhin, Incommensurate magnetic order and phase separation in the two-dimensional Hubbard model with nearest- and next-nearest-neighbor hopping, Phys. Rev. B **81**, 094407 (2010).

[31] J. Lorenzana, C. Castellani, and C. Di Castro, Phase separation frustrated by the long-range Coulomb interaction. I. Theory, Phys. Rev. B **64**, 235127 (2001).

[32] A. Bianconi, N. Poccia, A. Sboychakov, A. Rakhmanov, and K. Kugel, Intrinsic arrested nanoscale phase separation near a topological Lifshitz transition in strongly correlated two-band metals, Supercond. Sci. Technol. **28**, 024005 (2015).

[33] The long-range Coulomb interaction is not explicitly present in our model. Such a simplistic treatment is justified provided that the relative strength of the Coulomb interaction is sufficient to suppress completely the tendency toward the phase separation. In systems with large Δ_0 and a soft lattice (that is, a large dielectric constant due to lattice screening $\varepsilon_{\text{latt}} \gg 1$), this condition may be violated, and the study of an emergent inhomogeneous state will require a more elaborate approach.